Supplementary Information

Asymmetrically Tipped MoS_2/CdS Heterostructure for High-Performance Photocatalytic Plastic Reforming

Yu Yao[a], Jinqiang Zhang[a,*], Panpan Zhang[b], Lei Shi[c], Kunsheng Hu[a], Tara Pukala[d], Yanlin Shi[e], Zhongfan Jia[e], Shaobin Wang[a], and Xiaoguang Duan[a,*]

[a] *School of Chemical Engineering, The University of Adelaide, Adelaide, SA 5005, Australia*

[b] *School of Chemistry and Chemical Engineering, Jiangsu University, Zhenjiang 212013, China*

[c] *College of Materials Science and Engineering, Nanjing Forestry University, Nanjing, Jiangsu, 210037 China*

[d] *School of Physics, Chemistry and Earth Sciences, The University of Adelaide, SA 5005, Australia*

[e] *Institute for Nanoscale Science and Technology, College of Science and Engineering, Flinders University, Bedford Park, South Australia 5042, Australia*

*Corresponding author: Jinqiang Zhang; Xiaoguang Duan

E-mail address: jinqiang.zhang@adelaide.edu.au (J. Zhang)

E-mail address: xiaoguang.duan@adelaide.edu.au (X. Duan)

This **Supplementary Information** include: **13** Pages, **11** Figures, and **6** References

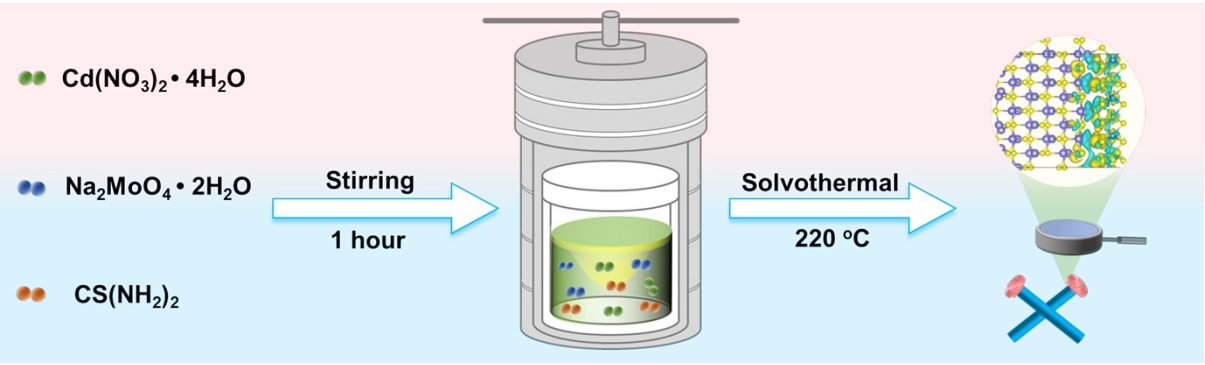

Fig. S1. Schematic diagram of the preparation of CdS and various x-MoS_2/CdS.

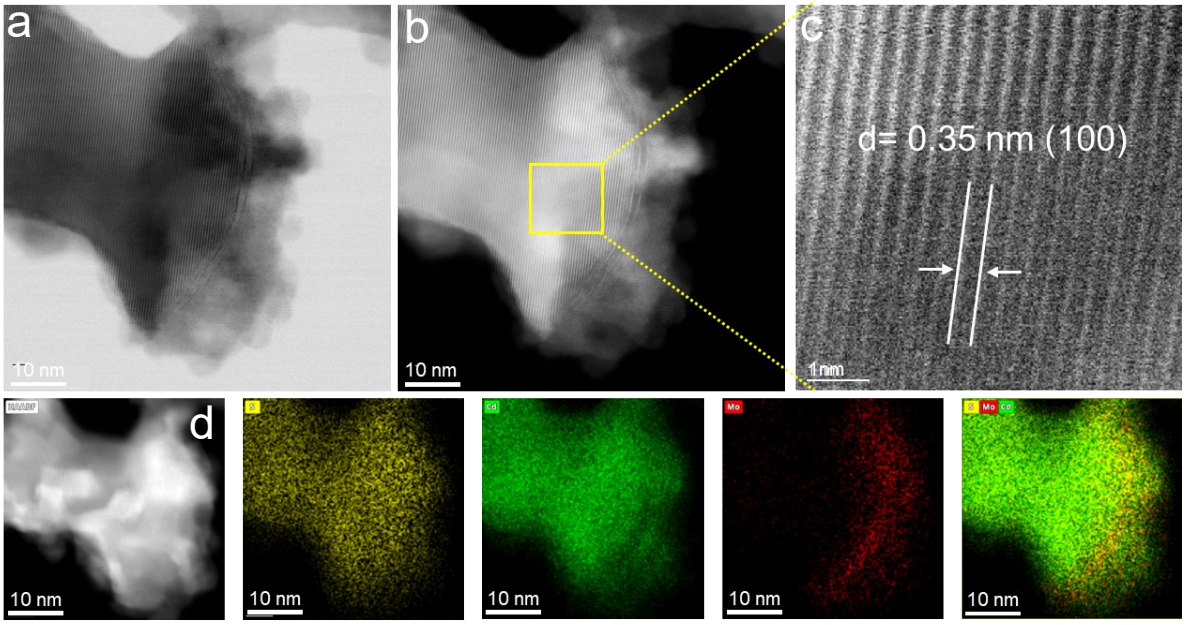

Fig. S2. Morphology of 3-MoS_2/CdS. (a) HRTEM and (b, c) HAADF-STEM images for 3-MoS_2/CdS. (d) HAADF-STEM and EDS mapping images of 3-MoS_2/CdS.

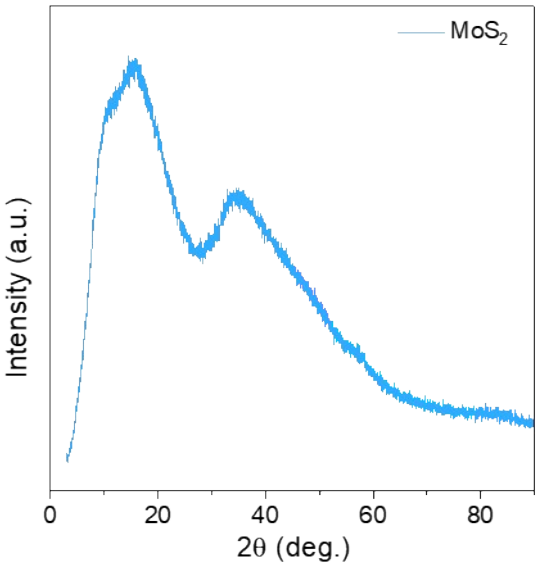

Fig. S3. XRD pattern of MoS_2.

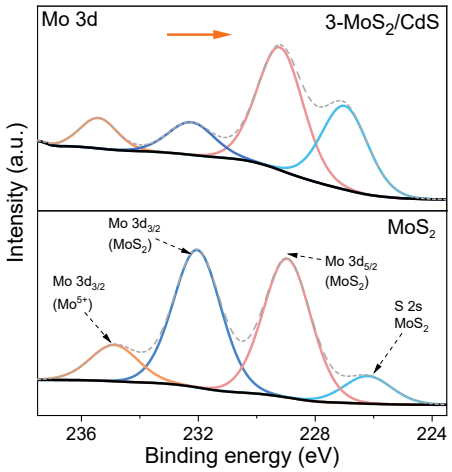

Fig. S4. Mo 3d XPS spectrum for CdS and 3-MoS_2/CdS.

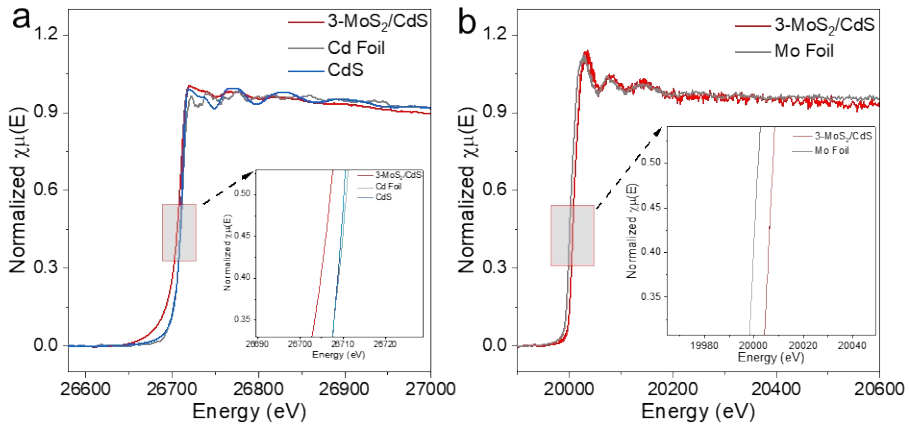

Fig. S5. XANES results. (a) Cd K-edge spectra of CdS, 3-MoS_2/CdS and reference samples. (b) Mo K-edge spectra of 3-MoS_2/CdS and reference samples.

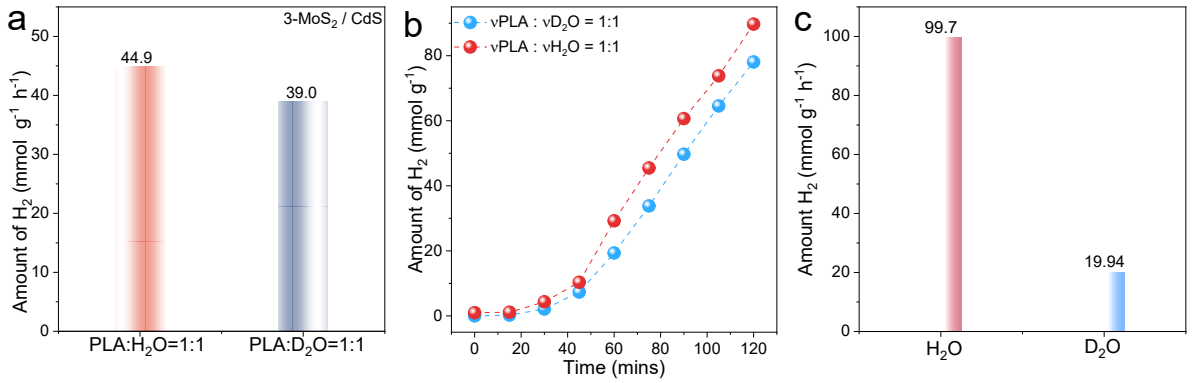

Fig. S6. (a-b) Time-dependent HER of 3-MoS_2/CdS in H_2O and D_2O under visible light irradiation, respectively. (c) Comparison of HER rates of 3-MoS_2/CdS catalyst between using H_2O and D_2O as media.

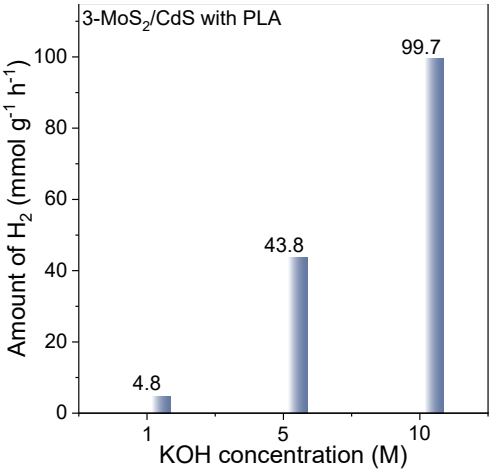

Fig. S7. H_2 generate rate for 3-MoS_2/CdS under the different KOH concentration pretreat PLA.

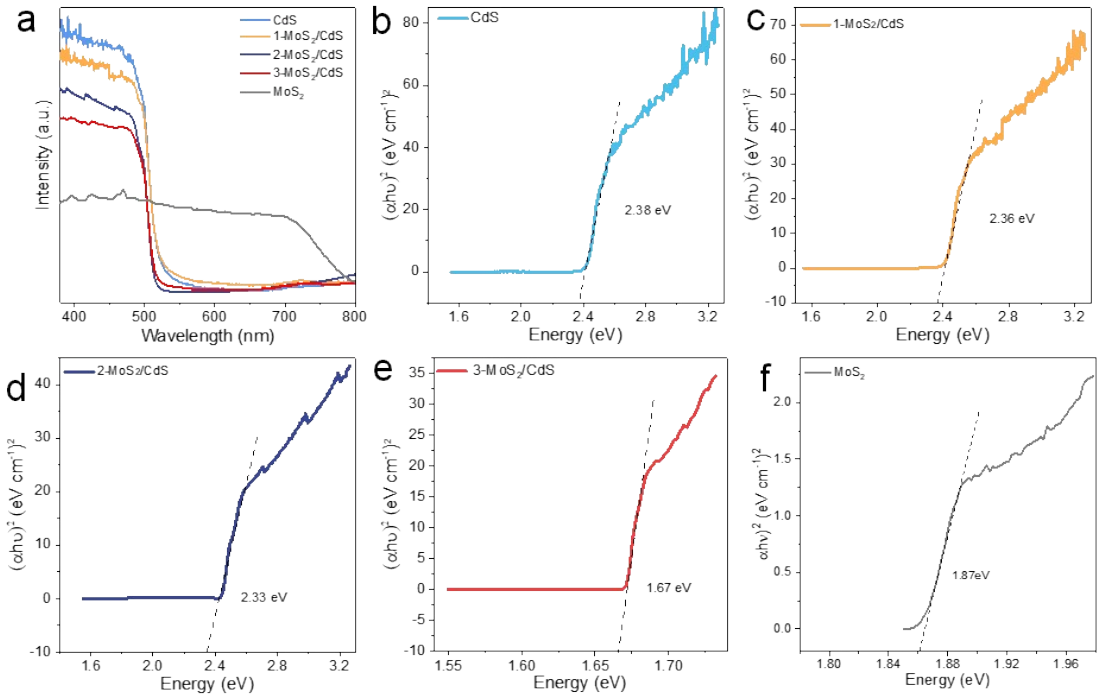

Fig. S8. (a) UV-Vis spectra and (b-f) estimation of bandgap for CdS, 1-MoS_2/CdS, 2-MoS_2/CdS, 3-MoS_2/CdS and MoS_2.

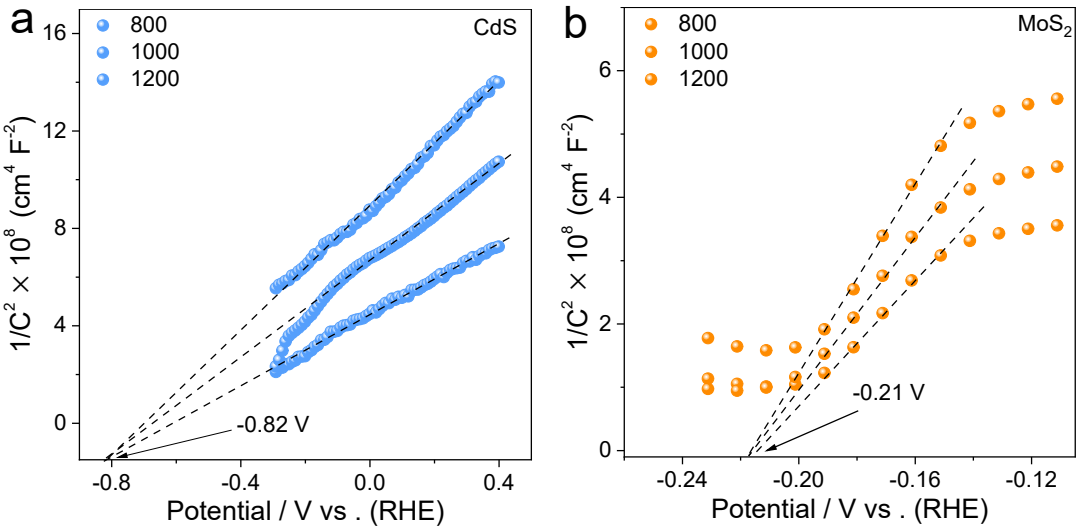

Fig. S9. Mott-Schottky curves of CdS and MoS_2.

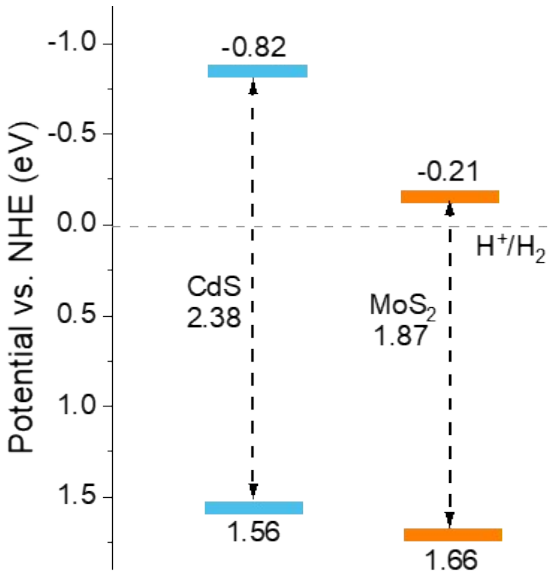

Fig. S10. Schematic for electronic band structure for CdS and MoS_2.

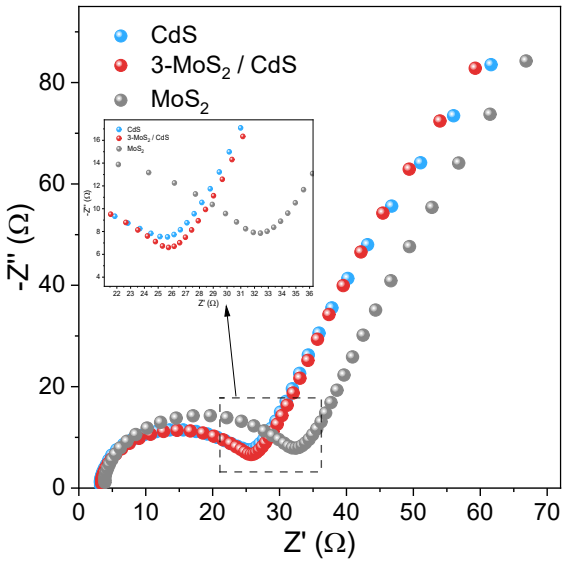

Fig. S11. EIS Nyquist plots of CdS, MoS_2 and 3-MoS_2/CdS.

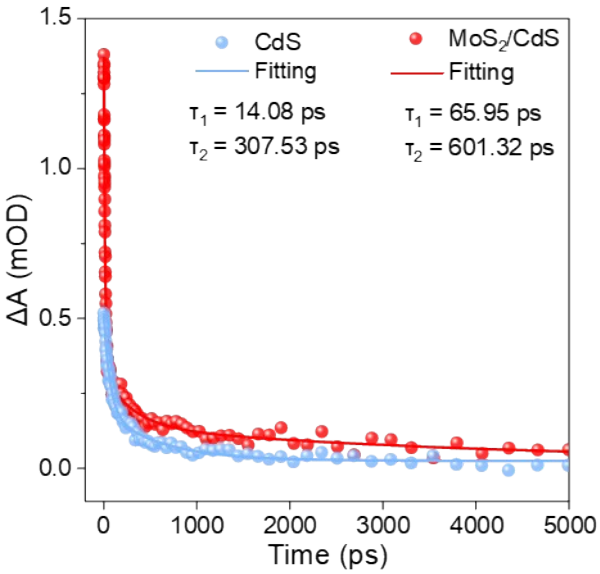

Fig. S12. Normalized decay kinetics and fitted curves of CdS and 3-MoS_2/CdS at 400 nm.

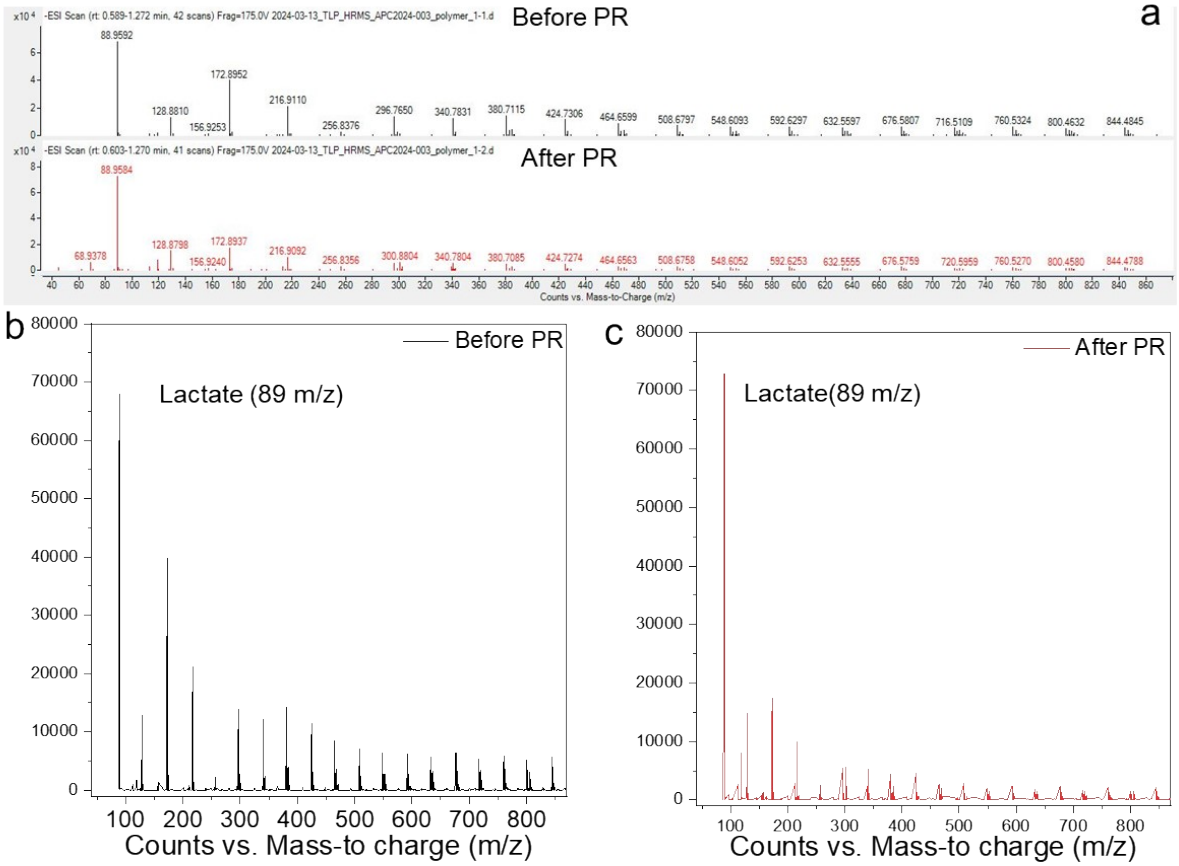

Fig. S13. (a) LC-MS spectrum of solubilized PLA components in 10 M KOH after pretreatment, corresponding to samples shown in (b) and (c). (b) Before PR; (c) After PR. The intensity at 89 m/z, attributed to lactate, increases after light irradiation, indicating the accumulation of lactate as a degradation product.

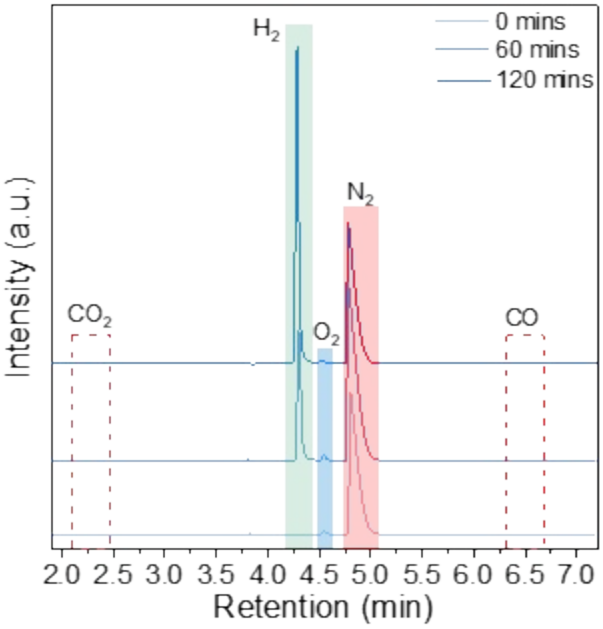

Fig. S14. Gas chromatography spectrum of the gaseous products generated from the photocatalytic depolymerization of PLA solution using the 3-MoS_2/Cd catalyst under light irradiation. The characteristic peaks corresponding to H_2, O_2, N_2, and CO_2 are indicated at 2 hours.

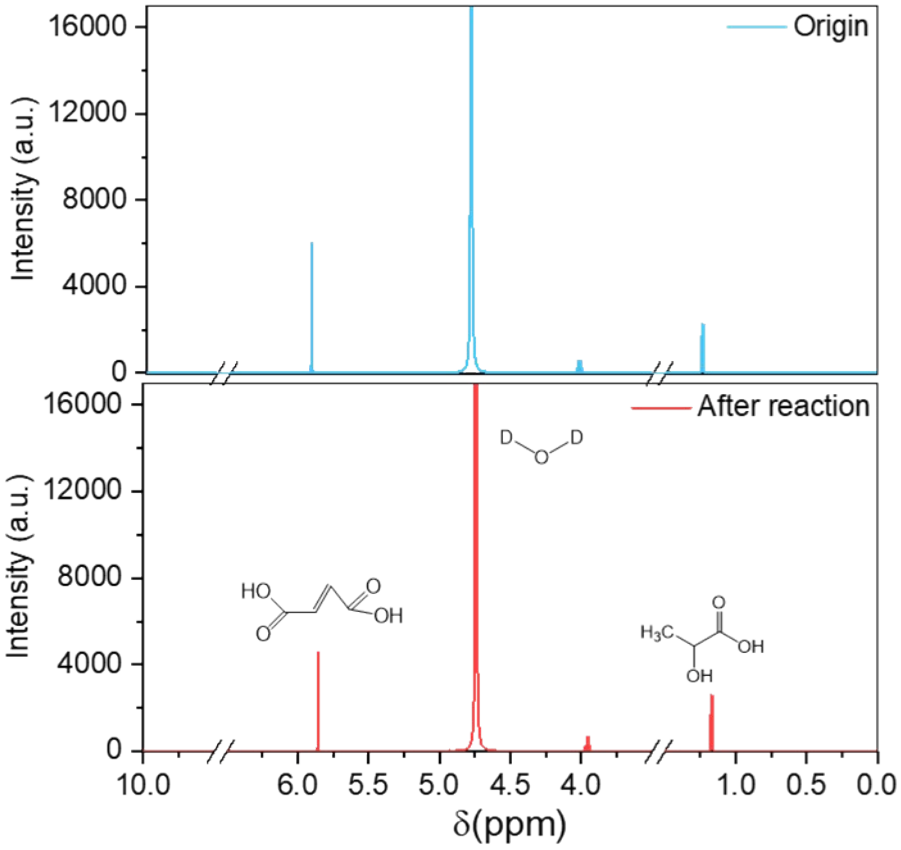

Fig. S15. ^{1}H NMR spectra for PLA pre-treated in 10 M KOH (upper) and that after 2 hours PR (lower).